CHEMISTRY
A European Journal

A Journal of
ChemPubSoc Europe

Accepted Article

Title: OFF-ON-OFF red-emitting fluorescence indicators for a narrow pH window

Authors: Antonin Cidlina, Miroslav Miletin, Mahtab Fathi-Rasekh, Victor Nemykin, Petr Zimcik, and Veronika Novakova

To be cited as: *Chem. Eur. J.* 10.1002/chem.201604978

Link to VoR: http://dx.doi.org/10.1002/chem.201604978

Supported by
ACES

WILEY-VCH

10.1002/chem.201604978

WILEY-VCH

FULL PAPER

OFF-ON-OFF red-emitting fluorescence indicators for a narrow pH window

Antonin Cidlina,[a] Miroslav Miletin,[a] Mahtab Fathi-Rasekh,[b] Victor Nemykin,*[b,c] Petr Zimcik,* [a] and Veronika Novakova,* [d]

Abstract: A unique combination of two independent mechanisms of fluorescence quenching, intramolecular charge transfer (ICT) from a peripheral donor and protonation of azomethine nitrogens in zinc tetrapyrazinoporphyrazines (TPyzPz) provides a new possibility for sensing pH in a specific range. The pH selectivity was controlled by the different basicities of the donor for ICT (dimethylaminoaryl), connected to the macrocycle by π-extended linkers of different lengths. ICT and protonation were studied in detail by photophysical, spectral (UV-Vis and MCD spectra) and electrochemical measurements that were further supported by theoretical calculations (DFT, TDDFT). The pH-sensing properties of the TPyzPzs were investigated in THF and in water after anchoring the TPyzPzs to liposomes. pK_a values were of ~1.3 (azomethine nitrogen) and 2.29-4.76 (donor for ICT). The lead indicators (sensing over a pH range of 1.0-2.5) with fairly steep sensing profiles exhibited increases in fluorescence between the OFF/ON states of more than 20 times and strong absorption in the red region (Q-band maximum > 650 nm, ε ~ 2×10^6 M^{-1} cm^{-1}).

Introduction

Since the establishment of the pH scale by Sørensen and the discovery of the first pH electrode in the beginning of the 20th century,[1] pH sensors have become essential in a wide range of applications in various fields such as medical diagnosis, biochemical and environmental analysis, and industrial applications, as well as in different research areas. Current trends involving miniaturization down to submicrometer dimensions, low cost and compatibility with mass-production methods make optical chemical pH sensors (*i.e.,* optodes) more useful than the well-established electrochemical pH sensor, which suffers from a susceptibility to electrical interference, an unsuitability for long-term measurements due to electrode signal drift and the necessity of a separate reference sensor.[2] Thus, the development of structurally-new pH indicators for optodes with improved properties in relation to the generally used fluorescein and coumarin derivatives is highly appreciated.

Tetrapyrazinoporphyrazines (TPyzPzs), aza-analogues of phthalocyanines (Pcs)[3, 4] with an extended 18 π-conjugated macrocyclic system absorb and emit light in the red region (above 650 nm, ε ~ 2×10^6 M^{-1} cm^{-1}). TPyzPzs possess many properties common to Pcs, such as strong fluorescence, chemical stability and fine tuning of optical and electrochemical properties by peripheral substitution.[5] On the other hand, the unique strongly electron deficient[6] character of the TPyzPz core predestines them for specific applications where Pcs cannot be used. In recent years, TPyzPzs have become effective fluorescence indicators for either metal cations[7] or pH[8-10] based on the ultrafast intramolecular charge transfer (ICT) or photo-induced electron transfer (PET) between a donor (*e.g.*, peripheral amine or phenolate) and acceptor (*i.e.*, macrocyclic core).[11] For detailed descriptions of the principles of ICT- or PET-based indicators, readers are encouraged to read the excellent reviews[12].

An interesting strategy that may result in higher selectivity at particular pH values involves the development of sensors operating on the OFF-ON-OFF principle, *i.e.*, using pH indicators turned on at only selected pH values. Reports of only few such indicators have been published to date, with the principles based mostly on the presence of two different donors for PET[13] or on changing the overall charge using various micelles[14]. However, all these published molecular switches suffer from emission in only the UV area. To the best of our knowledge, only two examples of OFF-ON-OFF indicators emitting in the red region of the spectrum have been published, and only recently. One describes indicators lacking a narrow pH-sensitive window (4.0-15.0, experiments made in DMSO)[15], and the second project focused on indicators suitable over a basic pH range, with rather low fluorescence enhancement when the indicators are switched ON[10]. In this project, we designed pH-driven OFF-ON-OFF indicators for an acidic pH range using two completely different switching mechanisms available in TPyzPzs, *i.e.*, ICT switching at the peripheral donor amine and protonation of the azomethine nitrogen. The idea is that the fluorescence switches ON when the proton concentration is increased but switches OFF again as the acidity increases further (Figure 1). Thus, strong fluorescence is expected at only intermediate pH values, leading to a narrow pH-sensing window. Notably, the protonation of the azomethine nitrogen has been mentioned in the literature to lead to a substantial decrease in the fluorescence quantum yields of both

[a] A. Cidlina, M. Miletin, P. Zimcik
Department of Pharmaceutical Chemistry and Pharmaceutical Analysis, Faculty of Pharmacy in Hradec Kralove, Charles University in Prague, Heyrovskeho 1203, Hradec Kralove, 500 05, Czech Republic, E-mail: petr.zimcik@faf.cuni.cz
[b] M. Fathi-Rasekh, V. Nemykin
Department of Chemistry and Biochemistry, University of Minnesota, Duluth 1039 University Drive, Duluth, MN 55812, USA,
[c] V. Nemykin
Department of Chemistry, University of Manitoba, Winnipeg, MB R3T 2N2, Canada. E-mail: victor.nemykin@umanitoba.ca
[d] V. Novakova
Department of Biophysics and Physical Chemistry, Faculty of Pharmacy in Hradec Kralove, Charles University in Prague, Heyrovskeho 1203, Hradec Kralove, 500 05, Czech Republic E-mail: veronika.novakova@faf.cuni.cz, web: http://portal.faf.cuni.cz/Groups/Azaphthalocyanine-group/

Supporting information for this article is given via a link at the end of the document.

Pcs and TPyzPzs[16-19] but has never been used as a concept in molecular switches or logic gates.

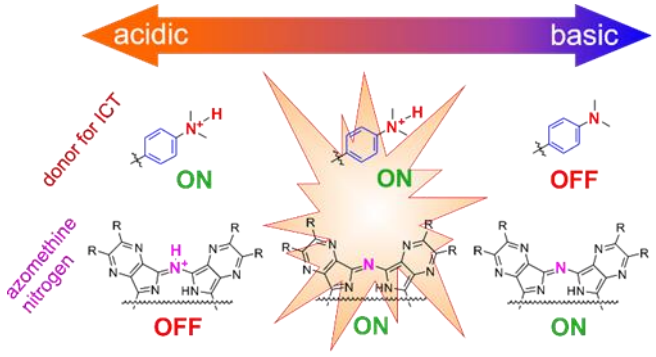

Figure 1. Proposed principle of OFF-ON-OFF switching of fluorescence

Hence, a series of TPyzPzs **1** – **4** with an *N,N*-dimethylamino group attached to π-conjugated linkers of different lengths was designed (Scheme 1). Compound **5** with a donor connected through a three-atom aliphatic linker was included in the study for comparison of ICT and PET. The peripheral substitution (*tert*-butylsulfanyl substituents) of the TPyzPz macrocycle as a whole series was chosen to suppress the undesirable formation of H-aggregates[20] and, together with the central zinc cation, to ensure good photophysical properties after activation of the indicator to the ON state.

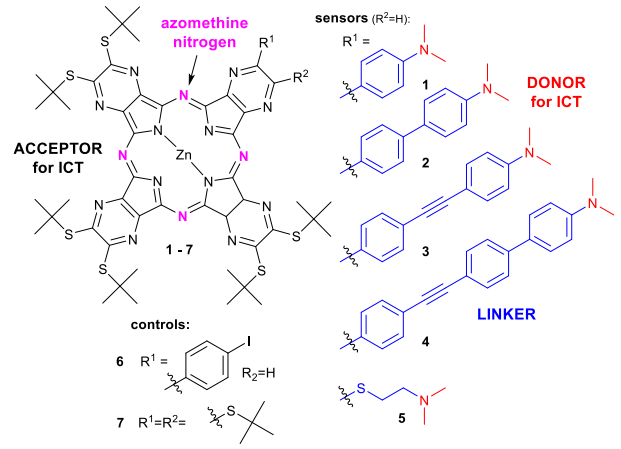

Scheme 1: Structures of the target indicators 1-5 and controls 6 and 7.

Results and Discussion

Synthesis

Generally, the synthesis of TPyzPzs is performed by cyclotetramerization of precursors, typically 5,6-disubstituted pyrazine-2,3-dicarbonitriles. Based on the atom connecting the peripheral substituent, different synthetic approaches are used for the synthesis of the desired precursors.[4] Thus, alkylheteroatom-substituted **19** and **20**[21] were prepared *via* nucleophilic substitution with *N,N*-dimethylaminoethanethiolate and *tert*-butanethiolate, respectively (Scheme 2). Compound **19** was converted directly to its hydrochloride and stored in this form because of the rapid decomposition typical of similar precursors containing aliphatic tertiary amines.[22]

The Suzuki-Miyaura cross-coupling reaction of halides **13** and **14** with boronic esters **8**-**10** was used for the synthesis of precursors with peripheral substituents connected *via* C-C bonds (Scheme 2). Synthon **13** was prepared by condensation of glyoxylic acid with diaminomaleonitrile (DAMN) in acetic acid with subsequent chlorination with $POCl_3$ according to a previously published procedure.[23] Similarly, compound 14 was obtained as a product of the condensation of DAMN with 2-(4-iodophenyl)-2-oxoacetaldehyde, which was prepared by partial oxidation of 4-iodoacetophenone with selenium dioxide. The optimization of the reaction conditions of the Suzuki-Miyaura cross-coupling reactions is summarized in Table 1.

Interestingly, the use of a bidentate ligand catalyst, $Pd(dppf)Cl_2$, was found to be crucial in the coupling reaction of pyrazine **13** with pinacol boronate **8** to obtain precursor **15** in a reasonable yield of 59%. A similar observation has been reported by McKillop et al.[24] using 2-chloropyrazine. On the other hand, lower yields were always obtained in the synthesis of **16**-**18** using this catalyst in comparison with $Pd(PPh_3)_2Cl_2$ in the reaction of the iodo-substituted synthon **14** with the appropriate pinacol boronates **8**-**10** (Table 1).

The synthesis of unsymmetrical TPyzPz was accomplished by cyclotetramerization of two different precursors (A and B) in a ratio of 3:1 under Linstead conditions (Scheme 3).[3] The statistical condensation of precursors A (**20**) and B (**14**-**16** or **19**), initiated by magnesium butoxide, led to the formation of a mixture of six congeners (AAAA, AAAB, AABB, ABAB, BBBA and BBBB), of which the AAAB type was of interest. The mixture of magnesium complexes was hardly separable from each other due to strong tailing on silica. Therefore, the mixture was directly converted to the corresponding metal-free derivatives upon treatment with *p*-TsOH in THF, and the desired metal-free AAAB congeners were chromatographically isolated and obtained in reasonable yields of 8 - 13%.

Table 1. Conditions of Suzuki-Miyaura cross-coupling reactions[a]

Starting material	Product	Catalyst	Yield
13	**15**	$Pd(PPh_3)_2Cl_2$	0 %
13	**15**	$Pd(dppf)Cl_2$	59 %
14	**16**	$Pd(PPh_3)_2Cl_2$	53 %
14	**16**	$Pd(dppf)Cl_2$	25 %
14	**17**	$Pd(PPh_3)_2Cl_2$	86 %
14	**17**	$Pd(dppf)Cl_2$	79 %
14	**18**	$Pd(PPh_3)_2Cl_2$	43 %
14	**18**	$Pd(dppf)Cl_2$	35 %

[a] Reaction conditions: **13** or **14** (1 eq.), appropriate derivative of pinacol boronate **8** – **10** (1.3 eq.), K_2CO_3 (2 eq.), Pd catalyst (5 mol%), 80 °C, THF/H_2O (4:1) (v/v), 7 h, under an argon atmosphere.

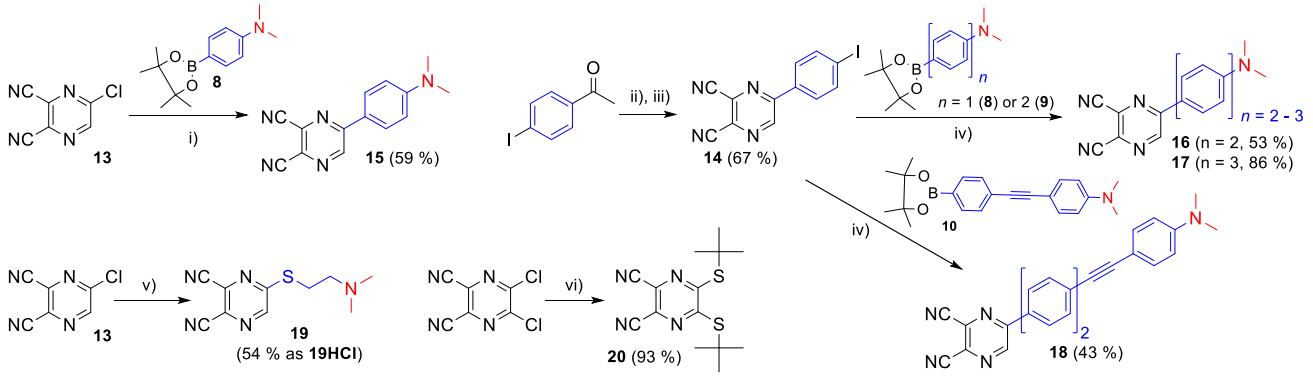

Scheme 2: Synthetic pathways for the precursors. Reaction conditions: i) $Pd(dppf)Cl_2$ (0.05 equiv.), K_2CO_3 (2 equiv.), THF/H_2O (4:1) (v/v), 7 h, 80 °C, Ar atmosphere. ii) SeO_2, dioxane/H_2O (2:1) (v/v), reflux, 12 h. iii) DAMN, AcOH, 3 h, reflux. iv) $Pd(PPh_3)_2Cl_2$ (0.05 equiv.), K_2CO_3 (2 equiv.), THF/H_2O (4:1) (v/v), 7 h, 80 °C. v) 2-(dimethylamino)ethanethiol hydrochloride, K_2CO_3, DMSO, 30 min, rt. vi) 2-methyl-2-propanethiol, NaOH, THF, 15 min, rt.

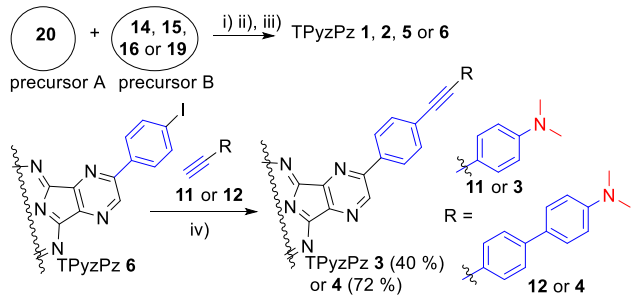

Scheme 3: Synthetic pathways for TPyzPzs. Reaction conditions: i) $Mg(BuO)_2$, BuOH, reflux, 8 h. ii) *p*-TsOH, THF, rt, 1 h. iii) $Zn(OAc)_2$, pyridine, reflux, 1 h. iv) appropriate acetylene **11** or **12** (2 equiv.), $Pd(PPh_3)_2Cl_2$ (0.03 equiv.), CuI (0.03 equiv.), PPh_3 (0.02 equiv.), triethylamine (4 equiv.), 48 h, room temperature, anhydr. THF, Ar atmosphere.

Finally, zinc complexes **1**, **2**, **5** and **6** were prepared from the corresponding metal-free derivatives by their heating with anhydrous zinc acetate in pyridine, with yields of the final conversion step between 74 - 92%.

The corresponding cyclotetramerization of precursors **20** (A) with **17** or **18** (B) failed due to the extremely low solubility of precursors **17** and **18** in all common solvents, and a different approach had to be employed for the synthesis of TPyzPzs bearing longer π-conjugated linkers. Thus, 4´-iodophenyl-substituted TPyzPz **6** was chosen as a suitable intermediate for further post-cyclotetramerization modification by the cross-coupling reaction (Scheme 3). However, the Suzuki-Miyaura cross-coupling reactions of **6** with synthons **8** or **9** gave only traces of the desired products using either $Pd(dppf)Cl_2$ or $Pd(PPh_3)_2Cl_2$ as the catalysts. For this reason, the structures of the target TPyzPzs with longer π-conjugated linkers were modified to enable the use of Sonogashira instead of Suzuki-Miyaura cross-coupling, and the appropriate TPyzPzs **3** and **4** were prepared by coupling TPyzPz **6** with ethynyl derivatives **11** or **12** in yields of 40% and 72%, respectively. Notably, successful post-cyclotetramerization modifications of the Pc[25] or TPyzPz[26] core under Sonogashira cross-coupling conditions have rarely been described in the literature.

UV-Vis and MCD spectra

First, the UV-Vis spectra of compounds **1**–**7** were measured in dichloromethane (DCM). It was found that the majority of new compounds form a significant amount of aggregates in this solvent, as indicated by the appearance of a broad band at the lower-energy side of the Q-band. However, The UV-Vis and MCD spectra of the same compounds in THF, pyridine or DCM/pyridine (99.5:0.5 v/v) systems have band widths in the Q-band region that are typical of monomeric phthalocyanines and their analogues. All prepared compounds of the series exhibited characteristic absorption bands in their UV-Vis and MCD spectra (Figures 2 and S1) typical of TPyzPzs (*i.e.*, a high-energy B-band at 377 - 379 nm and a low-energy Q-band at 647 - 656 nm, Table 2). It is interesting to note that the addition of the conjugated peripheral π-system to compounds **1**-**4** did not affect the energy of the Q-band in these systems compared to the reference, symmetric TPyzPz **7**, which indicates that the electronic effects of the new peripheral substituents in **1**–**4** are close to the cumulative effects of the alkylsulfanyl groups in **7**. Moreover, in all asymmetric zinc TPyzPzs **1**-**6**, the Q-band remains unsplit, which is indicative of their effective four-fold symmetry. In agreement with this observation, a very strong Faraday MCD A-term associated with the corresponding Q-bands was observed in the UV-Vis spectra of **1**-**6**. Another Faraday MCD A-term was observed in the B-band region of all target compounds and is typical of the symmetric TPyzPzs.[27] Finally, a rather weak and broad negative MCD signal in **1**-**6** is associated with the broad unstructured absorption in the 420 - 500 nm region, which will be discussed in detail in the computational section. Thus, the UV-Vis and MCD spectra of the target asymmetric TPyzPzs **1**-**4** suggest that the influence of the dimethylaminoaryl-containing substituent on the energies of the TPyzPz-core centered π–π* transitions is rather small, which correlates well with the electrochemical and DFT data discussed below.

Table 2. Absorption, photophysical and electrochemical properties of the investigated TPyzPzs in THF[a]

TPyzPz	λ_{max}	λ_{em}	Φ_Δ	Φ_F	$\Phi_\Delta + \Phi_F$	E^1_{ox} (V)	E^2_{ox} (V)	E^1_{red} (V)	E^2_{red} (V)
1	656	663	0.029	0.006	0.035	1.01	1.35	-0.56	-0.73
2	652	660	0.037	0.016	0.053	0.92	1.31	-0.54	-0.72
3	651	659	0.038	0.019	0.057	1.00	1.38	-0.58	-0.76
4	650	658	0.079	0.041	0.12	0.89	1.33	-0.54	-0.66
5	647	653	0.32	0.19	0.51	1.19	1.31	-0.55	-0.69
6	649	655	0.62	0.31	0.92	1.32	-	-0.51	-0.66
7	650	656	0.56	0.34	0.89	1.33	-	-0.69	-

[a] Absorption maximum at the Q-band (λ_{max}), fluorescence emission maximum (λ_{em}), fluorescence quantum yield (Φ_F), singlet oxygen quantum yield (Φ_Δ), half-wave reduction potential (E_{red}), and half-wave oxidation potential (E_{ox}). Φ_F and Φ_Δ are expressed as the mean of three independent measurements; estimated error ±15%. Potentials E_{red} and E_{ox} are expressed as $E_{1/2}$ (in V vs. SCE) with Fc/Fc^+ as an internal standard.

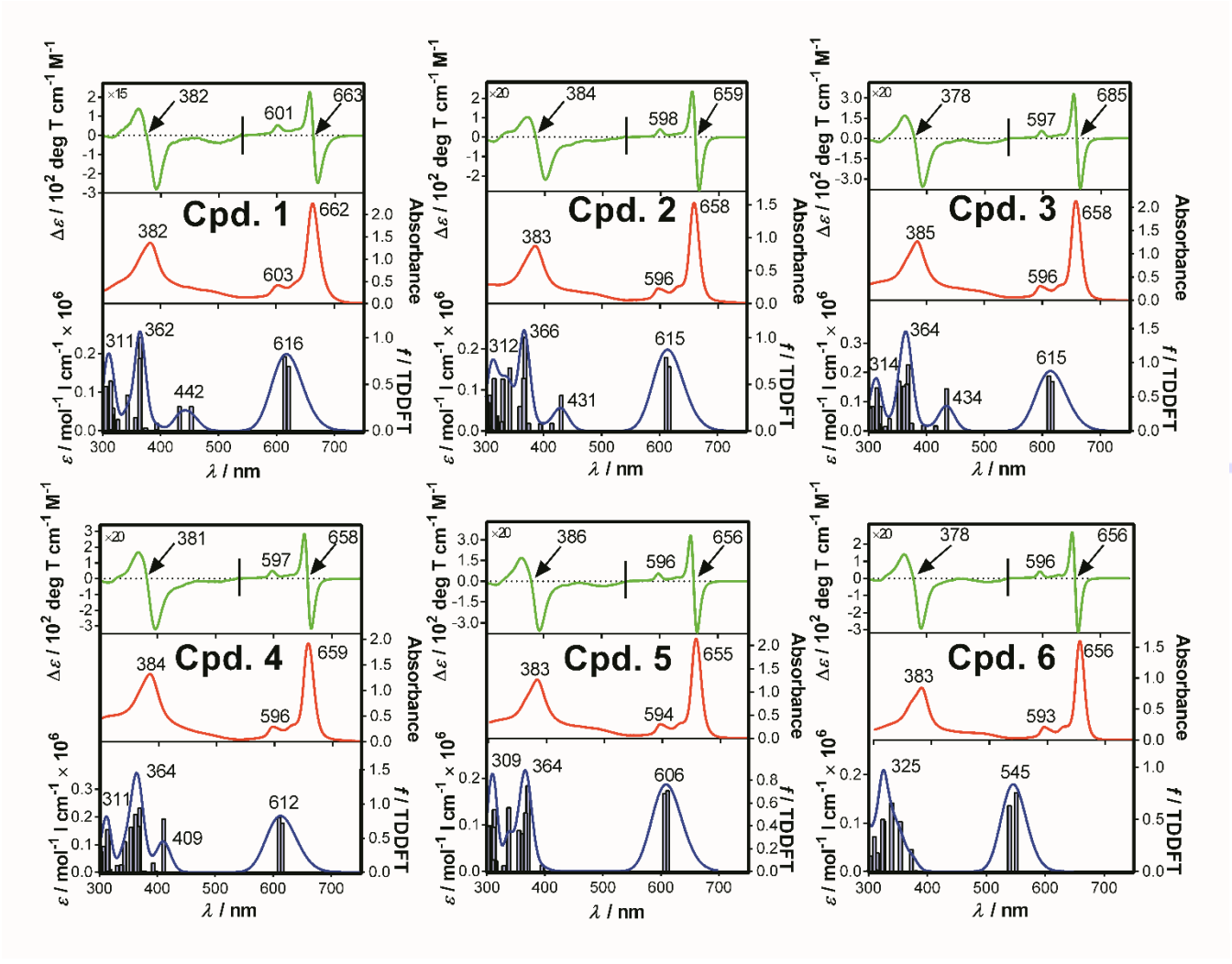

Figure 2. MCD spectra (green, upper graph) in a DCM/pyridine system; experimental UV-Vis spectra (red, middle graph) and TDDFT-PCM (blue, lower graph) of asymmetric compounds **1**–**6** in a pyridine system.

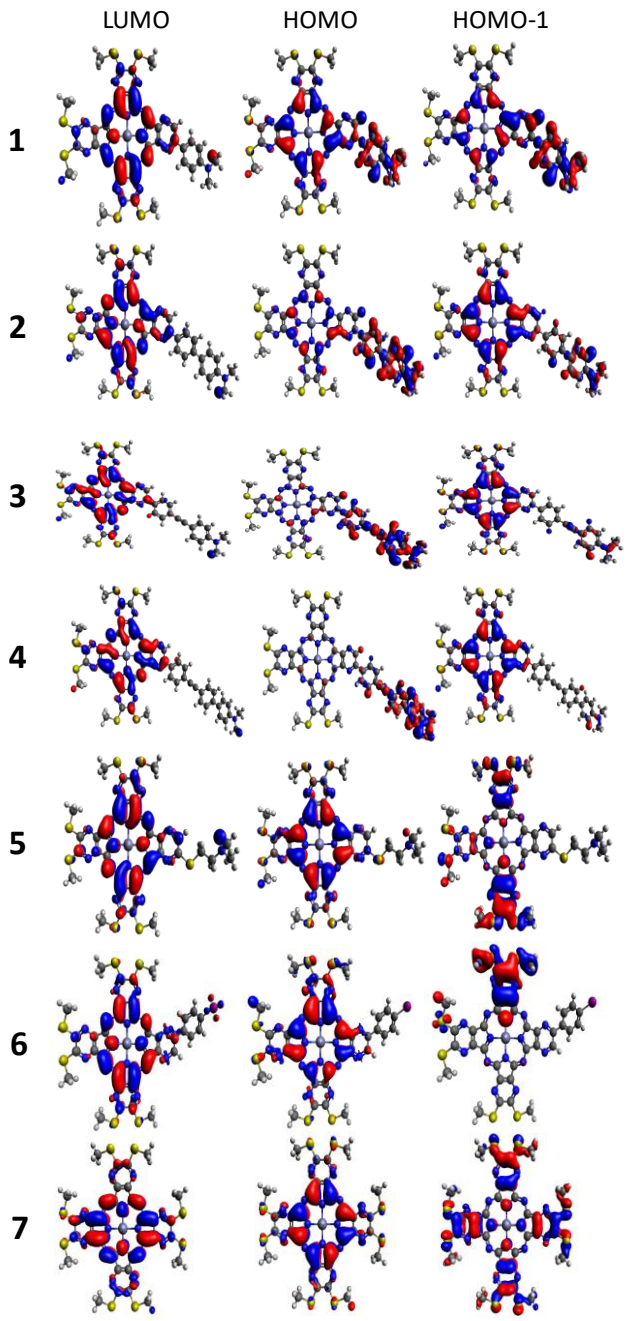

Figure 3. Selected DFT-predicted orbitals of compounds **1**-**7**.

DFT and TDDFT calculations

In order to explain the observed optical, photophysical, and redox properties of the new asymmetric compounds **1**-**5** in comparison to the symmetric reference compounds **6** and **7**, their electronic structures and the nature of the excited states were probed by DFT and TDDFT methods coupled with the polarized continuum model (PCM) approach to account for the solvent effect. CAM-B3LYP was used to account for the long-range ICT transitions in the TDDFT calculations. The DFT-predicted frontier orbitals are shown in Figure 3, the energy diagram for asymmetric systems **1**-**6** and reference compound **7** is given in Figure 4, and the orbital compositions of all target compounds are shown in Figure S3. DFT

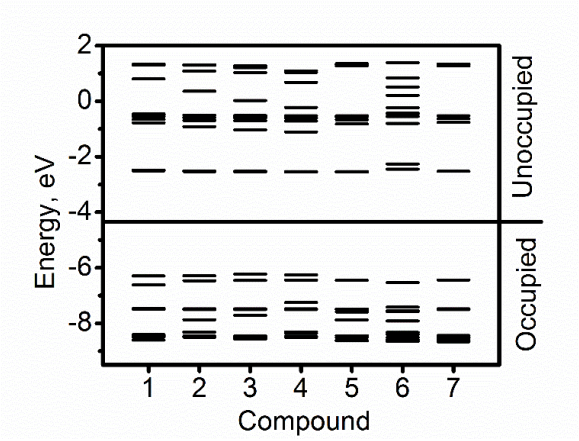

Figure 4. DFT-predicted orbital energy diagram for asymmetric compounds **1**-**6** and reference compound **7**. (A) Frontier orbital energies; (B) selected orbital energies for the most important orbitals.

predicted that the LUMO and LUMO+1 in all compounds are centered at the aromatic macrocycle and are nearly degenerated in all amino group-containing systems (**1**–**5**), as well as in reference compound **7**. Indeed, the energy difference between the LUMO and the LUMO+1 in asymmetric compounds **1**-**5** does not exceed 0.02 eV, which explains the presence of a single unsplit Q-band in these compounds (see TDDFT discussion below). The macrocycle-centered nature of the LUMO also explains the similarity between the spectroscopic signatures of the single-electron reduced compounds **1**, **2**, **3**, and **5** obtained under spectroelectrochemical conditions. The energy difference between the LUMOs of the individual compounds **1**-**5** (~0.05 eV) is also rather small and correlates well with the small difference (40 mV) in their first reduction potential. The DFT-predicted nature of the HOMO in asymmetric compounds **1**–**6**, as well as in reference system **7**, allows explanation of their photophysical properties. Indeed, the HOMO in **1** has a large (~30%) contribution, whereas the HOMO in **2**-**4** is dominated (~75 - 90%) by a contribution from the dimethylaminoaryl fragment. The HOMO in TPyzPz **1** is ~0.3 eV higher in energy than the predominantly peripheral group-centered HOMO-1. In contrast, the HOMO in asymmetric systems **5** and **6** as well as reference compound **7** should resemble the classic Gouterman's a_{1u} orbital expected for a normal tetraazaporphyrin core. DFT also predicted that such a Gouterman's a_{1u} orbital in TPyzPzs **2**–**4** is the HOMO-1 (Figures 3 and S3). The presence of the redox-active, diaminoaryl-centered HOMO in **2**–**4** and closely spaced HOMO and HOMO-1 in **1** creates an opportunity for ICT process in these compounds but not in systems **5**-**7**. As a result, one might expect that the fluorescence should be severely suppressed only in systems **1**-**4**, in excellent agreement with the experimental photophysical data (see below).

Moreover, DFT predicted that the first oxidation in compounds **1**-**4** should be centered at the peripheral substituents but the first oxidation process in systems **6**-**7** should be macrocycle-centered, in agreement with the electrochemical data. Another interesting

observation is that the increase in the -NMe_2 group-to-macrocycle distance results in a higher degree of localization of the HOMO at the peripheral substituent, which correlates with a minor increase in the fluorescence quantum yield. Indeed, the HOMO of **1** resembles Gouterman's a_{1u} orbital with high (32%) contamination from the dimethylaminophenyl group. This orbital is closely followed by HOMO-1, which is slightly (56%) dominated by a contribution from the peripheral substituent. The HOMO in **2**-**4** is predominantly localized on the peripheral substituent, whereas the closely spaced (0.17 - 0.22 eV) HOMO-1 is almost purely a Gouterman's type macrocycle-centered a_{1u}. The lack of conjugation between the -NMe_2 group and an aromatic macrocycle in asymmetric system **5** results in a situation where the localization on this fragment MO was predicted to be the well-stabilized HOMO-4, although CAM-B3LYP calculations might underestimate its energy. The DFT-predicted energies of the HOMOs in all tested compounds correlate with their first oxidation potential determined by electrochemical methods. Taking into consideration that the nearly degenerate LUMO and LUMO+1 are macrocycle-centered, one might expect that some of the ICT band be present in the low-energy region of the UV-Vis spectra of compounds **1**-**4** but not system **5**. The TDDFT calculations of all target compounds in comparison with their experimental spectra are shown in Figure 2. Indeed, the TDDFT-predicted ICT energy increases in the following order: **1** < **2** ~ **3** < **4** << **5** (453, 430, 435, 411, and 294 nm, respectively), and this order correlates very well with the experimentally observed fluorescence quantum yields and the singlet oxygen generation capability of compounds 1-5 (Figure 5). Thus, one might speculate that, in the simplified approach, an energy of the ICT transition would dictate the efficiency of the fluorescence quenching and the singlet oxygen production (*i.e.*, the lower the ICT energy, the stronger fluorescence quenching and the lower singlet oxygen production ability that specific compound would possess).

In addition to the ICT bands in compounds **1**-**5**, TDDFT predicted classic macrocyclic π–π* transitions, which are responsible for the most intense bands in the Q- and B-regions of all studied symmetric and asymmetric macrocyclic systems. Indeed, in all TPyzPzs **1**-**7**, the first two excited states are dominated by the Gouterman's macrocycle-centered a_{1u} (HOMO or HOMO-1) → LUMO, LUMO+1 single electron excitations and are predominantly π–π* in nature. Similarly, the most intense transitions in the B-band region predicted by TDDFT are dominated by the macrocycle-centered π–π* single-electron excitations from the HOMO-n to LUMO, LUMO+1.

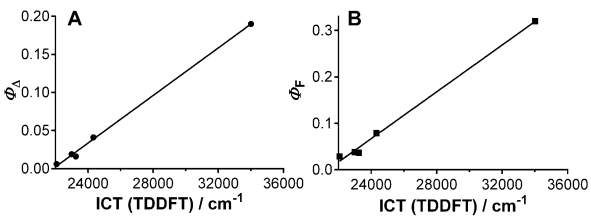

Figure 5. Correlation of the singlet oxygen (A) and fluorescence quantum yields (B) of **1-5** with the TDDFT predictions.

Electrochemistry and spectroelectrochemistry

The electrochemical data were obtained from cyclic voltammetry and square wave voltammetry in THF at room temperature. Appropriate E_{red} and E_{ox} were determined from square wave voltammetry (Table 2) using ferrocene (Fc/Fc^+) as an internal standard and tetrabutylammonium hexafluorophosphate as a supporting electrolyte.

The aminogroup-containing TPyzPzs **1**–**5** underwent two reductions (Figure S2). The E^1_{red} and E^2_{red} were almost equal in **1**–**5** (~ -0.55 V and ~ -0.70 V vs. SCE). These values correlate well with the values of the structurally close control **6** (-0.51 and -0.66 *V* vs. SCE) but were slightly different from E^1_{red} of symmetrical **7** (-0.69 *V* vs. SCE, similar to the value published previously[27]). This result may indicate spreading of the π-conjugated system on the peripheral aryl moiety. However, due to the small difference from the value of **7**, the presence of a *π*-extended peripheral substituent is not believed to significantly affect the electron-accepting properties of the TPyzPz core.

Two irreversible oxidations were observed for **1**-**5**. The E^2_{ox} values of **1**–**5** in the range of 1.31 – 1.38 V vs. SCE can be assigned to the oxidation of the TPyzPz core because of the similar values observed for control compounds **7** and **6** (1.33 and 1.32 V vs. SCE respectively). In addition to the oxidation of the core, another oxidation process with E^1_{ox} = 0.89-1.01 V vs. SCE was detected for aminoaryl-bearing compounds **1**–**4** as a consequence of oxidation of the amine moiety, which is in accordance with the DFT predictions. This oxidation did not occur for controls **6** and **7**. The E^1_{ox} values differed only slightly within the series, suggesting a comparable electron-donating ability of the amine for ICT. A similar trend in E_{ox} values was recently described by Bures et al. for dialkylamino-substituted pyrazine-2,3-dicarbonitriles substituted with various π-extended linkers.[28] Noticeably, a different value of E^1_{ox} for the amino group was observed only for TPyzPz **5**, *i.e.,* a model compound of the PET process, which is simply explained by the aliphatic character of the donor amine.

To gain insight into the nature of the redox-generated species in asymmetric systems **1**-**5**, a set of spectroelectrochemical experiments was conducted in a pyridine/tetrabutylammonium perchlorate (TBAP) system. Because the first oxidation process in all systems and the first reduction process in **4** were found to be irreversible, only the first reduction processes were studied for compounds **1**, **2**, **3**, and **5**. In addition, spectroelectrochemical reduction of reference compound **7** was previously discussed by our group[27]. The choice of the pyridine/0.3 M TBAP system was dictated by an increased stability of the electrochemically generated anion-radicals of the target compounds in pyridine. Similar experiments conducted in THF, DMF, and DCM/pyridine systems resulted in a fast decomposition of the reduced species under spectroelectrochemical conditions. Since an influence of the dimethylamino group on the energies of π–π* transitions in asymmetric systems **1**-**5** was found to be negligible and, as was shown by the DFT calculations, the LUMO in **1**-**5** is macrocycle-centered. Therefore, it is not surprising that the reduction of compounds **1**, **2**, **3**, and **5** under spectroelectrochemical conditions led to a very similar transformation of their UV-Vis spectra dominated by the TPyzPz-core-centered π–π* excitations (Figure 6). In particular, during reduction of compounds **1**, **2**, **3**, and **5** under spectroelectrochemical conditions, the Q-band disappeared; the B-band was reduced in intensity; and two new absorption bands formed at approximately 440 and 550 nm, along with a very characteristic and broad new band in the NIR region

between 750 and 1000 nm. Because of the broad nature of the NIR band, a peak at ~830 nm was identified for all compounds, while a structural peak at ~900 nm was also observed in the case of reduced compounds **3** and **5**. The transformations of the UV-Vis spectra of asymmetric systems **1**, **2**, **3**, and **5** were very close to the spectroscopic signatures of reference compound **7** reduced under spectroelectrochemical conditions and are clearly indicative of the single-electron reduction of the TPyzPz core.

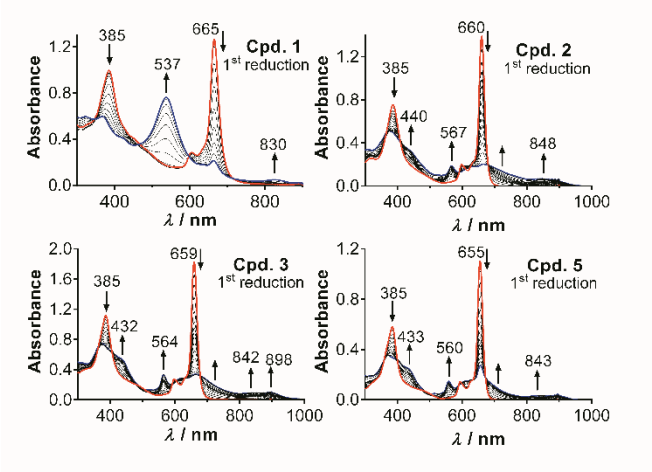

Figure 6. Spectroelectrochemical transformation of the neutral compounds **1-3** and **5** during the first reduction in the pyridine/0.3 M TBAP system.

Photophysical measurements and ICT efficiency

Singlet oxygen quantum yields (Φ_Δ) were determined in THF using a singlet oxygen quencher, 1,3-diphenylisobenzofuran, and unsubstituted zinc Pc as a reference ($\Phi_{\Delta(THF)}$ = 0.53[29]). Fluorescence quantum yields (Φ_F) were determined in THF after excitation in the Q-band region (λ_{exc} = 595 nm) with zinc Pc as a reference ($\Phi_{F(THF)}$ = 0.32[5]). These data are summarized in Table 2. The emission spectra featured a shape typical of TPyzPzs, mirroring the appropriate absorption spectra with a typical small Stokes shift (~ 7 nm). The excitation spectra perfectly matched the absorption spectra, which confirmed the presence of only monomeric species; therefore, the determined quantum yields were not affected by undesirable aggregation (Figure S4).

Because ICT and PET are competitive relaxation pathways to singlet oxygen production and fluorescence emission, the sum of the quantum yields ($\Phi_\Delta + \Phi_F$) may give reliable information about the efficiency of ICT or PET. Obviously, the values of Φ_Δ and Φ_F of **1** – **4** are one order of magnitude lower than those of the controls **6** and **7**, not exceeding 0.08 and 0.04 for Φ_Δ and Φ_F, respectively (Figure S5). These results prove the excellent efficiency of ICT, which increased in a series of **4** << **3** ~ **2** < **1**, which is in accordance with the TDDFT predictions (Figure 5). As the oxidation ability of the donors in TPyzPzs **1**-**4** is comparable to the measured E^1_{ox} values (see Table 2), the increase in the ICT efficiency can be clearly attributed to the shortening of the π-conjugated linker.

The particular quantum yields of **5** were less suppressed, giving the sum ($\Phi_\Delta+\Phi_F$) = 0.51 and fully in accordance with the TDF prediction and values determined for similar compounds[30]. Of note is that the distance between the dimethylamino group (donor for ICT) and the macrocycle (acceptor) is comparable in **1** and **5**. The extremely different photophysical data of these two compounds therefore emphasizes the importance of conjugation between the donor and acceptor on the quenching efficiency. Both controls **6** and **7** reached high values of both quantum yields (Table 2), with sums of $\Phi_\Delta + \Phi_F$ close to 1. The slightly higher Φ_Δ and lower Φ_F of 6 containing an iodo substituent may be clearly explained by the heavy atom effect, according to which the introduction of heavy atoms into the molecule supports the relaxation of excited states through intersystem crossing.[31]

Generally, the feasibility of ICT is improved in a polar medium that stabilizes the charge-separated state and, conversely, is suppressed in a non-polar medium.[32] To further characterize the impact of ICT in the investigated compounds, the Φ_F of **2** was determined in a series of solvents of different polarity. In some cases, 1% pyridine was added to the solution to suppress undesirable aggregation. Such an amount of pyridine was believed not to influence the final polarity of the investigated solvent. The obtained Φ_F values were plotted as a function of the relative permittivity (ε_r) of the solvent (Figure S6, Table S1). The lowest Φ_F of 0.004 was observed in DMSO (ε_r = 48.9). On the contrary, the ICT was not as effective in non-polar benzene (ε_r = 2.2), in which Φ_F reached a value of 0.19. The Φ_F of **2** clearly correlated with the polarity of the medium, as the feasibility of ICT increased in more polar solvents. The significant differences in Φ_F demonstrate the high sensitivity of ICT in the tested TPyzPz systems and the possibility of its control in a desired manner.

pH sensing – OFF-ON-OFF fluorescence switching

Contrary to all routinely used indicators that operate on a simple ON-OFF principle, sensing in a narrow pH window requires two quenching mechanisms that must closely cooperate and for which switching must occur at approximately similar pH values. In this work, we chose the ICT process from a peripheral donor and quenching based on protonation of azomethine nitrogens.

Since all target indicators **1**-**5** possess the same macrocyclic core, quenching by protonation of the azomethine nitrogens proceeds at identical pH (or at identical c_{TFA}, see below) for the whole series, and the sigmoidal branches at lower pH are virtually coincident. Therefore, the pH sensing range may be tuned by the use of different donors for ICT. The ICT efficiency and the basicity of the donor amine are the two most important parameters to consider to acquire fluorescence indicators with high sensitivity and selectivity. The ICT efficiency determines the difference in fluorescence intensity between ON/OFF states (*i.e.,* signal-to-noise ratio), while the donor basicity controls the pH range in which the switching to the ON state occurs. Both the sensitivity and selectivity of TPyzPzs **1**-**5** to pH and acid concentration in organic solvent (including controls **6** and **7**) were investigated by the mean of the fluorescence measurements, firstly in THF upon stepwise addition of trifluoroacetic acid (TFA) and then in water in buffers of different pH. The results are summarized in Table 3 and depicted in Figure 7.

The addition of TFA into THF solutions of indicators **1**-**5** led to protonation of the peripheral donor amine, being the most basic center in the studied TPyzPzs. Protonation of the dimethylamino group did not affect the absorption spectra but was accompanied by a significant increase in fluorescence intensity (up to 19 times) due to suppression of ICT. The progress of the protonation driven by the basicity of the particular donor was characterized by the equilibrium constants for association of TFA with *N*,*N*-

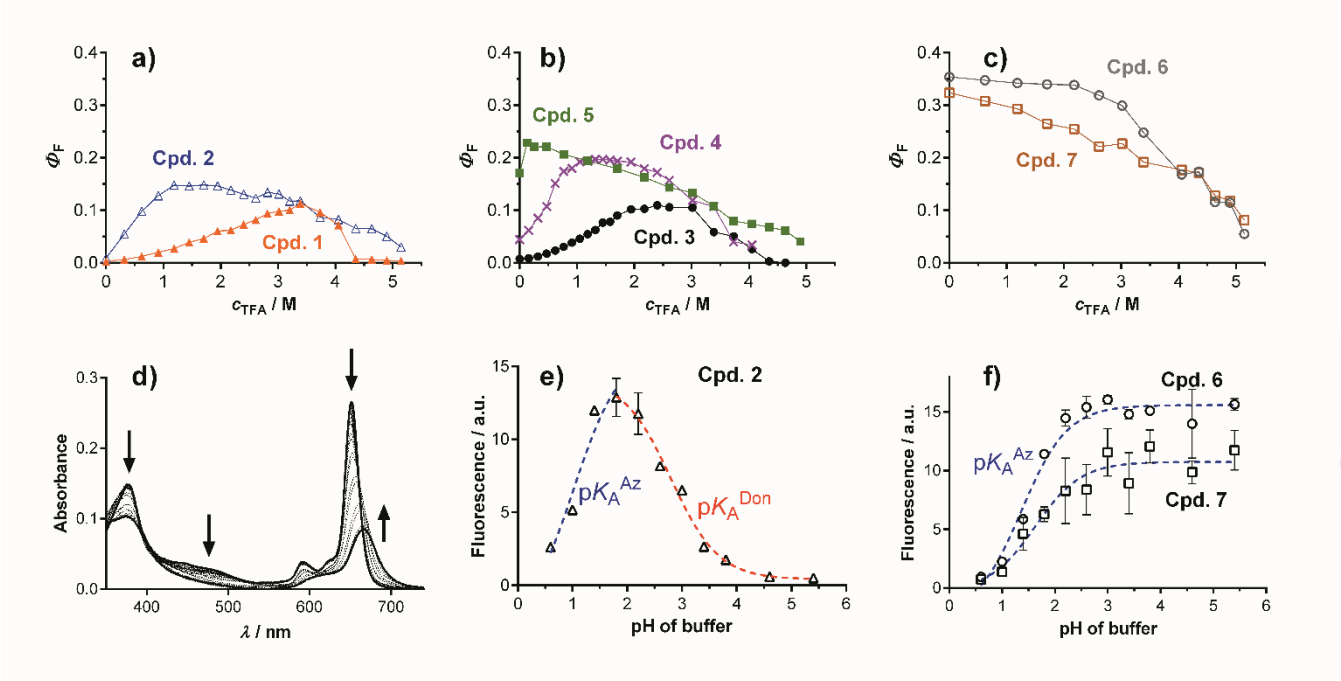

Figure 7. Study of the pH-sensitive properties of the investigated compounds: a-c) changes in Φ_F of **1**-**7** in THF upon addition of TFA; d) changes in the absorption spectra of **2** in THF upon addition of TFA (c_{TFA} = 0-5 mol/L); and e-f) changes in the fluorescence intensity of **2**, **4**, **6** and **7** after their incorporation into the DOPC liposomes in buffers of different pH (λ_{exc} = 375 nm). The mean of three independent measurements.

dimethylamino group of TPyzPz in THF (K^{Don}). Considering the values of K^{Don}, the basicity of the donors decreased in the series **5** >> **4** > **2** ~ **3** > **1**. The fluorescence enhancement factor (FEF, *i.e.,* ratio between the fluorescence in the OFF/ON states) of ICT-based indicators **1**-**4** showed promising values, ranging from 5.8 - 19.0 when going from 0 to approx. 2.5 mol/L TFA in solution. The difference in FEF was caused primarily by the dissimilar quenching efficiency of ICT in the OFF states (see above). Expectedly, **5** bearing a strongly basic aliphatic alkylamino group reached a maximum of Φ_F, even under slightly acidic conditions, but with only a weak increase in fluorescence intensity (only 1.2×). Therefore, PET does not appear to be a very suitable process for the development of TPyzPz-based pH indicators.

Table 3. pH sensing properties of indicators **1**-**5** and comparison to controls **6** and **7** [a]

Cpd.	$\Phi_{F\,max}$	K^{Az} [M^{-1}]	K^{Don} [M^{-1}]	pK_A^{Az}	pK_A^{Don}
	THF	THF	THF	H_2O	H_2O
1	0.11	0.26	0.55	- [b]	2.29
2	0.18	0.26	0.90	1.02	2.89
3	0.11	0.28	0.81	- [b]	3.18
4	0.20	0.31	1.09	1.11	2.57
5	0.23	0.28[c]	- [b]	1.61	4.76
6	0.31	0.26		1.37	
7	0.34	0.32		1.63	

[a] ^{Don} values for protonation of the peripheral donor amine; ^{Az} values for protonation of azomethine nitrogens; [b] not possible to determine; [c] determined from the decrease in the Q-band maxima in the absorption spectrum.

Even if the FEF was quite high for **1**-**4**, the Φ_F in the ON state (0.11-0.20) did not reach the possible maximum values determined for controls **6** and **7** without possible ICT/PET (Φ_F of 0.31 and 0.34, respectively). This result can be clearly explained by the concomitant protonation of the second basic center at higher TFA concentrations, the azomethine nitrogens, *i.e.*, the appearance of the second quenching mechanism involved in these OFF-ON-OFF indicators.

In accordance with the literature, protonation of the azomethine nitrogens was accompanied by a significant decrease in fluorescence.[11, 16-18] The Φ_F values of the azomethine-protonated species dropped to zero, indicating that this quenching process is extremely efficient. Although the exact mechanism of this quenching has not yet been described, some authors have suggested that it might be attributed to an increased internal conversion pathway.[18] In addition to its effect on fluorescence intensity, the protonation of azomethine nitrogens can also be monitored by the characteristic decrease in absorbance in the Q-band area with the formation of a new red-shifted band[33] (Figure 7d, S7). The effect of protonation of the azomethine nitrogens on the fluorescence intensity is simply documented by the controls **6** and **7** (Figure 7c), which also enabled its full characterization by the association constants of TFA with azomethine nitrogen of TPyzPz (K^{Az} = 0.26 and 0.32 M^{-1} in THF, respectively). The K^{Az} values of the other compounds (**1**-**5**) in this series were found to be very similar (Table 3) and corresponded well with the values of K^{Az} determined from changes in the absorption spectra (Table S2). The obtained data are in good agreement with the results of the electrochemical measurements and TDDFT calculations that suggested a limited influence of amino group-bearing substitution on the electron density of the core and consequently on the

basicity of the azomethine nitrogens. Of note is that a slightly higher K^{Az} value was determined previously for analogous zinc octakis(*tert*-butylsulfanyl)phthalocyanine (0.53 M^{-1} in THF[16]), which is in accordance with its less electron-deficient core.

The abovementioned experiments in organic solvent prove that the combination of ICT blocking from a peripheral donor together with the protonation of azomethine nitrogens occurring with rather similar *K* values (compare K^{Az} and K^{Don}, Table 3) may lead to the development of a new class of indicators that are sensitive to a specific amount of acid in organic solvents or to specific pH range, *i.e.*, operating on the OFF-ON-OFF principle. It is interesting to note that the compounds can be used as fluorogenic indicators for acids in organic solvents, in a manner similar to recently reported multicolorimetric indicator for acid-base equilibrium in DCM.[34] Despite the fact that the abovementioned OFF-ON-OFF switching in THF showed quite promising results, pH sensing is most often applied in biological-friendly environments; therefore, the behavior of the studied TPyzPzs had to be demonstrated in aqueous conditions. Hence, compounds **1**–**5** and controls **6** and **7** were anchored to liposomes, which are considered a simple model of biological membranes[35], and the fluorescence intensity was studied in buffers with pH ranging from 0.6 to 5.4 (or up to 7.8 for the more basic compound **5**). Liposomes have been demonstrated to be suitable delivery systems that maintain *tert*-butylsulfanyl-substituted TPyzPzs in monomeric form, *i.e.*, the photophysically active form.[9] The results are shown in Figures 7e, f and S8. A similar biphasic character of the fluorescence dependence on pH to that displayed in THF was observed in the buffers for indicators **1**-**5**, whereas an increase in fluorescence reaching a plateau at ~pH > 3 was detected only for **6** and **7**. The acidity constants of the conjugated acids pK_A^{Az} (azomethine nitrogen) and pK_A^{Don} (dimethylamino group) could be determined in most cases. pK_A^{Az} values of approximately 1.5 (Table 3) were calculated for the azomethine nitrogens in **5**-**7**, whereas lower values were observed for **2** and **4**, for which the determination most likely suffers from concomitant donor protonation. To the best of our knowledge, this is the first report of pK_A values for the azomethine nitrogens in Pc and analogous compounds to date.

The apparent pK_A^{Don} values of the donor indicate the following order of donor basicity: **1** < **4** ~ **2** ~ **3** << **5**, with pK_A values ranging from 2.29 - 4.76. Determination of the pK_A values for the least basic compounds may, however, suffer from concomitant protonation of the azomethine nitrogens, which is why these values cannot be considered absolute. However, it is clear that all the sensors **1**-**5** were selectively sensitive to a narrow pH range (see Figures 7d and S7) with a promisingly high difference between the ON and OFF states, particularly for compounds **1** and **2** (FEF higher than 25 when going from neutral to pH~1.5 and 2.0, respectively).

Conclusions

The aim of this project was to develop pH indicators operating with the OFF-ON-OFF principle for specific pH ranges. Hence, a series of target pH indicators **1**-**4** operating on the ICT principle was prepared together with a PET-based indicator **5** and two controls **6** and **7**.

Photophysical, spectral and electrochemical measurements, which were further supported and explained by theoretical calculations, described in detail the ICT phenomenon of TPyzPzs **1**-**5**. In summary, the first oxidation in **1**-**4** proceeds at the peripheral donor but is macrocycle-centered in **6**-**7**. Further, the HOMO is less delocalized (more centered) at the peripheral donor group with the increasing length of the π-extended linker, which results in their lower ICT efficiency. This is in accordance with the TDDFT-predicted increase in the ICT band energy in the series **1** < **2** ~ **3** < **4** << **5**. The longer π-linker between the peripheral donor amine and TPyzPz core serving as an acceptor was undoubtedly found to decrease the ICT efficiency, which was clearly evident in the sum of $\Phi_\Delta+\Phi_F$; TPyzPz **1** was completely quenched by ICT, whereas **4** showed significantly retained fluorescence and singlet oxygen production. PET quenching (in TPyzPz **5**) was found to be less suitable for the development of fluorescence indicators based on TPyzPzs.

ICT-quenched TPyzPzs **1**-**4**, especially **1** and **2**, behaved as interesting pH indicators at acidic pH, operating with the OFF-ON-OFF principle by employing a combination of ICT quenching from the dimethylamino group and quenching by protonation of the azomethine nitrogens, which was clearly demonstrated in both organic solvent and water. The apparent *K* (using TFA in THF solutions of **1**-**7**) and pK_A (in water) values were determined for the protonation of the azomethine nitrogens in the TPyzPzs and the donor moieties.

Indicators **1** and **2**, sensitive to a pH range of 1.0-2.5 with fairly steep profiles and FEF higher than 20, are considered the promising candidates for further usage in fluorescence sensor devices. Their high impact in this area is also supported by the fact that these TPyzPz indicators possess strong absorption in the red region (Q-band maximum > 650 nm) with high extinction coefficients (ε ~ 2×10^6 M^{-1} cm^{-1}), resulting in high brightness of the sensors in the ON state, which is a particularly critical parameter in the case of fast-responding pH sensor devices. Moreover, the fluorescence emission in the red region (in contrast to the majority of available sensors operating only in the UV region) offers significant advantages in biological applications due to low light scattering, limited autofluorescence of endogenous chromophores, and high light penetration depth in tissues. As a consequence, indicators **1** and **2** belong among the candidates of pH indicators that may be further used in fluorescence sensor devices.

Acknowledgements

The work was supported by Czech Science Foundation (14-02165P), Charles University in Prague (SVV 260 291), Minnesota Supercomputing Institute and U of M Grant-in-Aid. Authors are grateful to Jiří Kuneš for NMR measurements, to Juraj Lenčo for measurements of MALDI-TOF MS and to Lucie Novakova for HRMS measurements.

Keywords: phthalocyanine • sensor • azomethine nitrogen • fluorescence • intramolecular charge transfer

[1] S. Sørensen, *Biochem. Zeit* **1909**, *21*, 131-200.

[2] D. Wencel, T. Abel, C. McDonagh, *Anal. Chem.* **2014**, *86*, 15-29.
[3] R. P. Linstead, E. G. Noble, J. M. Wright, *J. Chem. Soc.* **1937**, 911-921.
[4] M. P. Donzello, C. Ercolani, V. Novakova, P. Zimcik, P. A. Stuzhin, *Coord. Chem. Rev.* **2016**, *309*, 107-179.
[5] P. Zimcik, V. Novakova, K. Kopecky, M. Miletin, R. Z. Uslu Kobak, E. Svandrlikova, L. Váchová, K. Lang, *Inorg. Chem.* **2012**, *51*, 4215-4223.
[6] C. Bergami, M. P. Donzello, C. Ercolani, F. Monacelli, K. M. Kadish, C. Rizzoli, *Inorg. Chem.* **2005**, *44*, 9852-9861.
[7] L. Lochman, J. Svec, J. Roh, K. Kirakci, K. Lang, P. Zimcik, V. Novakova, *Chem.–Eur. J.* **2016**, *22*, 2417-2426; b) L. Lochman, J. Svec, J. Roh, V. Novakova, *Dyes Pigm.* **2015**, *121*, 178-187; b) V. Novakova, L. Lochman, I. Zajícová, K. Kopecky, M. Miletin, K. Lang, K. Kirakci, P. Zimcik, *Chem.–Eur. J.* **2013**, *19*, 5025-5028.
[8] J. P. Hill, N. K. Subbaiyan, F. D'Souza, Y. S. Xie, S. Sahu, N. M. Sanchez-Ballester, G. J. Richards, T. Mori, K. Ariga, *Chem. Commun.* **2012**, *48*, 3951-3953.
[9] V. Novakova, M. Miletin, K. Kopecky, P. Zimcik, *Chem.–Eur. J.* **2011**, *17*, 14273-14282.
[10] V. Novakova, M. Laskova, H. Vavrickova, P. Zimcik, *Chem.–Eur. J.* **2015**, *21*, 14382-14392.
[11] V. Novakova, P. Zimcik, M. Miletin, L. Vachova, K. Kopecky, K. Lang, P. Chábera, T. Polívka, *Phys. Chem. Chem. Phys.* **2010**, *12*, 2555-2563.
[12] J. F. Callan, A. P. de Silva, D. C. Magri, *Tetrahedron* **2005**, *61*, 8551-8588; b) J. R. Lakowicz, *Principles of fluorescence spectroscopy*, 3rd ed., Springer, New York, **2006**.
[13] G. J. Brown, A. P. de Silva, M. R. James, B. O. F. McKinney, D. A. Pears, S. M. Weir, *Tetrahedron* **2008**, *64*, 8301-8306; b) A. P. de Silva, H. Q. N. Gunaratne, C. P. McCoy, *Chem. Commun.* **1996**, 2399-2400.
[14] P. Pallavicini, Y. A. Diaz-Fernandez, L. Pasotti, *Analyst* **2009**, *134*, 2147-2152.
[15] S. Z. Topal, E. Onal, A. G. Gurek, C. Hirel, *Dalton Trans.* **2013**, *42*, 11528-11536.
[16] A. Cidlina, Z. Pausimova, M. Miletin, P. Zimcik, V. Novakova, *J. Porphyrins Phthalocyanines* **2015**, *19*, 1095-1106.
[17] A. O. Ogunsipe, M. A. Idowu, T. B. Ogunbayo, I. A. Akinbulu, *J. Porphyrins Phthalocyanines* **2012**, *16*, 885-894.
[18] A. Beeby, S. FitzGerald, C. F. Stanley, *J. Chem. Soc., Perkin Trans. 2* **2001**, 1978-1982.
[19] A. Beeby, S. FitzGerald, C. F. Stanley, *Photochem. Photobiol.* **2001**, *74*, 566-569.
[20] M. Kostka, P. Zimcik, M. Miletin, P. Klemera, K. Kopecky, Z. Musil, *J. Photochem. Photobiol., A* **2006**, *178*, 16-25.
[21] P. Zimcik, M. Miletin, V. Novakova, K. Kopecky, M. Nejedla, V. Stara, K. Sedlackova, *Aust. J. Chem.* **2009**, *62*, 425-433.
[22] P. Zimcik, M. Miletin, Z. Musil, K. Kopecky, L. Kubza, D. Brault, *J. Photochem. Photobiol., A* **2006**, *183*, 59-69.
[23] A. Nakamura, T. Ataka, H. Segawa, Y. Takeuchi, T. Takematsu, *Agric. Biol. Chem.* **1983**, *47*, 1555-1560.
[24] N. M. Ali, A. McKillop, M. B. Mitchell, R. A. Rebelo, P. J. Wallbank, *Tetrahedron* **1992**, *48*, 8117-8126.
[25] H. Ali, J. E. vanLier, *Tetrahedron Lett.* **1997**, *38*, 1157-1160; b) G. Bottari, D. D. Diaz, T. Torres, *J. Porphyrins Phthalocyanines* **2006**, *10*, 1083-1100; b) M. J. Cook, M. J. Heeney, *Chem.–Eur. J.* **2000**, *6*, 3958-3967; b) S. Osati, H. Ali, J. E. van Lier, *Tetrahedron Lett.* **2015**, *56*, 2049-2053; b) F. Dumoulin, H. Ali, V. Ahsen, J. E. van Lier, *Tetrahedron Lett.* **2011**, *52*, 4395-4397.
[26] V. Engelhardt, S. Kuhri, J. Fleischhauer, M. Garcia-Iglesias, D. Gonzalez-Rodriguez, G. Bottari, T. Torres, D. M. Guldi, R. Faust, *Chem. Sci.* **2013**, *4*, 3888-3893; b) S. Kuhri, V. Engelhardt, R. Faust, D. M. Guldi, *Chem. Sci.* **2014**, *5*, 2580-2588.
[27] V. Novakova, P. Reimerova, J. Svec, D. Suchan, M. Miletin, H. M. Rhoda, V. N. Nemykin, P. Zimcik, *Dalton Trans.* **2015**, *44*, 13220-13233.
[28] F. Bures, H. Cermakova, J. Kulhanek, M. Ludwig, W. Kuznik, I. V. Kityk, T. Mikysek, A. Ruzicka, *Eur. J. Org. Chem.* **2012**, 529-538.
[29] L. Kaestner, M. Cesson, K. Kassab, T. Christensen, P. D. Edminson, M. J. Cook, I. Chambrier, G. Jori, *Photochem. Photobiol. Sci.* **2003**, *2*, 660-667.
[30] V. Novakova, P. Hladik, T. Filandrova, I. Zajicova, V. Krepsova, M. Miletin, J. Lenco, P. Zimcik, *Phys. Chem. Chem.l Phys.* **2014**, *16*, 5440-5446.
[31] D. S. McClure, *J. Chem. Phys.* **1949**, *17*, 905-913; b) A. Harriman, *J. Chem. Soc., Faraday Trans.* **1981**, *77*, 1281-1291.
[32] L. Fajari, P. Fors, K. Lang, S. Nonell, F. R. Trull, *J. Photochem. Photobiol., A* **1996**, *93*, 119-128.
[33] V. Novakova, E. H. Mørkved, M. Miletin, P. Zimcik, *J. Porphyrins Phthalocyanines* **2010**, *14*, 582-591.
[34] A. Shundo, S. Ishihara, J. Labuta, Y. Onuma, H. Sakai, M. Abe, K. Ariga, J. P. Hill, *Chem. Commun.* **2013**, *49*, 6870-6872.
[35] R. R. C. New, ed., *Liposomes: a practical approach*, Oxford University Press, New York, **1990**.

Entry for the Table of Contents

Selective pH sensing: A unique strategy of sensing pH with a fairly steep sensing profile using red-emitting indicators from phthalocyanine family is described. Intramolecular charge transfer and protonation of azomethine nitrogens were shown to drive the sensing pH range. High brightness was achieved by strong absorption of indicator in the red region (Q-band maximum > 650 nm, ε ~ 2×10^6 M^{-1} cm^{-1}).

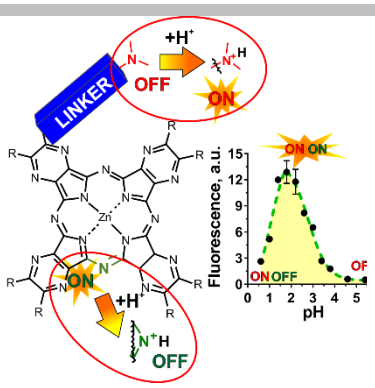

Antonin Cidlina, Miroslav Miletin, Mahtab Fathi-Rasekh, Victor Nemykin, Petr Zimcik,* Veronika Novakova,**

Page No. – Page No.

OFF-ON-OFF red-emitting fluorescence indicators for a narrow pH window